ANNALS OF GEOPHYSICS, 69, 2026; doi:10.4401/ag-9369
OPEN ACCESS

Machine learning approach to Nemrut Dağ and Bingöl obsidians: insights from Tūlūl al Baqarat obsidian prehistoric tools (Iraq, IV millennium BC) and volcanological implications

Gloria Vaggelli[*,1], Alessandro Borghi[2], Roberto Cossio[2], Stefano Ghignone[2], Carlo Lippolis[3]

(1) Istituto di Geoscienze e Georisorse, CNR, Via Valperga Caluso, 35, I-10123 Torino
(2) Dipartimento di Scienze della Terra, Università degli Studi di Torino, Via Valperga Caluso, 35, I-10123 Torino
(3) Dipartimento di Studi Storici, Università degli Studi di Torino, via Sant'Ottavio 20, I-10124 Torino

Article history: received May 16, 2025; accepted December 2, 2025

Abstract

A machine learning approach was employed to determine the source material of nine obsidian blades from the archaeological site of Tulūl al Baqarat (Iraq) employing geo-referenced obsidians from Nemrut Dağ stratovolcano and Bingöl volcanic plateaux as the reference dataset for the investigation. On the obsidian tools were performed chemical analysis using non-invasive and non-destructive techniques. Major and minor elements were determined using a low vacuum SEM-EDS microprobe, while trace elements were analyzed using a bench-to-top micro-XRF. To determine the provenance of obsidian artifacts and identify the volcanic complex from which the tools were sourced, through a comparative geochemical study, we used the chemical composition of georeferenced obsidian samples reported in literature. To minimize the differences related to different analytical techniques and different laboratory variability, we applied, for the first time, a machine learning approach. Indeed, in this study we demonstrated that only the machine learning approach proved an exhaustive method to discriminate and classify a dataset, complemented by well-known geochemical comparisons. The analyzed nine obsidian tools display a peraluminous rhyolite composition with a peculiar high Zr content which excludes most obsidian outcrops in Turkish and Armenian volcanic sites as potential original sources. Nevertheless, a machine learning approach applied to selected major, minor, and trace elements indicate the obsidian tools results comparable to Nemrut Dağ mild alkaline rhyolitic obsidians from pre-caldera eruptions. These obsidians are now exposed within the caldera and in Sicaksu outcrop (SE Türkiye). Therefore, the artifacts may even be attributed to specific Nemrut Dağ flows using geochemically significant elements. The provenance of the source from the Nemrut Dağ stratovolcano in south-eastern Türkiye, situated along the Turkish route of the Tigris River, supports the hypothesis of a network of trade and broad exchange since the 4th millennium BC, from southeastern Anatolia, which is presumed to have occurred along the Tigris River up to the shores of the Persian Gulf.

Keywords: Obsidian; Provenance; Machine learning; Bingöl; Nemrut Dağ

1. Introduction

Obsidian is an excellent natural row material widely used for making tools and precious objects by prehistoric people in Mediterranean area (Tykot, 1996) and in the Middle and Near East (Chataigner et al., 1998). When chipped, it creates exceptionally sharp and durable cutting edges thanks to its high hardness (5-5.5 on the Mohs scale) and conchoidal fracturing. To some extent, obsidian tools are better than chert and jasper for cutting softer materials like plants and animal flesh. Obsidian tools are also found in archaeological sites hundreds of kilometers away from their geological source (Tykot, 2002), even when alternative materials were available at minor distances, suggesting obsidians high value for ancient societies.

In archaeological reconstructions, obsidian tools play a significant archaeological and historical role for tracing the geological source and provenance by comparing chemical analysis with natural outcrops. This allows us to study interactions between different social or cultural groups, understand how obsidian use evolved over time, and examine the economic and social conditions associated with its usage and reconstruct route trade in the past.

The most common obsidian is black and has a rhyolitic composition (SiO_2 >70 wt.%) such as "Liparite", the well-known obsidian of Lipari (Aeolian Islands, Italy; Crisci et al., 1991), widely spread in the Mediterranean area in prehistoric times (Donato et al., 2018 and reference therein).

The chemical composition of obsidians based on the major elements allows them to be classified into main classes. The analysis of trace elements enables more detailed classifications, because it reflects different petrogenetic environments and whose abundances provide valuable insights into volcanic dynamics. This approach is particularly useful for classifying obsidian samples from different georeferenced outcrops, allowing or suggesting geological correlations.

This paper presents an archaeometric study on nine obsidians tools found in the Tulūl al Baqarat archaeological site, located in the province of Wasit, 180 km South-East of Baghdad in South-Central Iraq. The context of provenience of the studied tools is a rural settlement of the beginning-mid 4th millennium BC (Early Uruk period).

The provenance of obsidian artifacts was investigated through a comparative geochemical study, relying on the chemical composition of georeferenced obsidian samples reported in the literature Frahm, 2012, 2023). To minimize the influence of minor discrepancies arising from differences in analytical methods and laboratory variability, we employed, for the first time, a machine learning approach.

2. Archaeological and geological setting

Tulūl al-Baqarat is an archaeological site located on the Tigris River, 180 km South-East of Baghdad. Located on the eastern margins of the Mesopotamian alluvium, this area was important historically and has been inhabited over a long period (Lippolis, 2020). According to the survey carried out by the Italian expedition, the cultural layers attested in the area span from the 4th millennium BC (Early Uruk period) to the Islamic era (Lippolis, 2020). In antiquity, the region of Tulūl al-Baqarat was closer to the course of the Tigris River, and/or connected to it through a system of channels.

Tulūl al-Baqarat archaeological site consists of a rural settlement composed by ten mounds (tell in Arabic – tūlūl plural), whose main one is named TB1 (Tell Baqarat n. 1; Fig. 1a). This tell was extensively excavated from 2008 to 2010 by an Iraqi expedition with significant results (Fig. 1b; Bahar, 2020, 2022).

Between 2013 and 2022, the Italian expedition (sponsored by the University of Turin and the Centro Ricerche Archeologiche e Scavi di Torino) conducted soundings and a topographic survey on the main mounds of the area. Particular attention was given to a large low mound, named TB7 (Tell Baqarat n. 7; Fig. 1c), located approximately 1 km southeast of the previously mentioned TB1.

TB7 is a low tell, sized around eight hectares (Fig. 1d). To this extension should be added four hectares belonging to a second tell 200 m north-east of TB7, which was probably part of the same Uruk settlement.

The settlement shows a circular in shape and was delimited by a wide ditch, whose evidence is testified by a strong colour change between the inner part and the outer ring of land surrounding TB7.

TB7 architecture and other evidence point at dating the cultural layer to the main Early Uruk – Late Chalcolithic 2/3 period (4th millennium BC). Later historical phases (e.g., the Parthian period) are poorly documented, because of the strong erosion and land modifications that affected the site. Thus, TB7 contains the oldest evidence of human activity in the entire region (Lippolis, 2020).

Figure 1. Aerial views of the Tulūl al-Baqarat archaeological site: (a) TB1 biggest mount (tell); (b) TB1 archeological excavation; (c) TB7 mount: the site of provenance of the obsidian tools; (d) TB7 Italian archeological excavation area.

Despite this, small fragments of painted pottery are attributed to the late Obeid period, or to a transitional phase between Obeid and Uruk periods (4^{th}-5^{th} millennium BC). Obsidian tools studied in this paper were found in the TB7 tell. These items are a set of prehistoric tools of daily life, such as blades and splinters (Lippolis, 2020). Most of the obsidian tools found in TB7 tell come from a collection of surface contexts. Although present in the investigated levels, obsidians in excavated strata are rather rare compared to those encountered on the ground during a survey. However, it may be reasonable to claim that almost all the flints present in the tell can be attributed to the 4^{th} millennium BC cultural horizon (Lippolis, 2020).

2.1 The Anatolia obsidian source region

Obsidian sources in Western Mediterranean are very few and extensively studied, while in the Near East they cover hundreds of square kilometres with multiple eruptive phases recognized in most volcanic complexes. Moreover, besides major obsidian source areas, small outcrops are scattered across Anatolia. Consequently, this region has long posed challenges for precise obsidian source identification (Oddone et al., 2003). In recent years, however, significant progress has been made in developing comprehensive geochemical databases of Anatolian obsidians using different analytical techniques. In particular, thanks to the recent works by Frahm (2023, 2025), a much more up-to-date understanding of the geochemistry of Turkish obsidians, through detailed geochemical obsidian databases, is now available.

The obsidian source for Tūlūl al Baqarat tools could be sought in the obsidian-bearing volcanic areas which are easily accessible by the ancient populations and reachable by foot or by river transport. These characteristics are more relevant respect the proximity to the archaeological site wherein they are found, as suggested by Oddone et al. (2003). Anatolia, therefore, seems the most suitable area for obsidian provenance (see Frahm, 2023 and reference therein; Fig. 2a).

Anatolia is part of the Alpine-Himalayan orogenic belt, formed during the collision between Arabia-Africa and Eurasian plates, due to the closure of the Tethyan Ocean during the Mesozoic and Cenozoic (see e.g., Şengör and Yılmaz, 1981). During the Oligocene, the Arabia-Eurasia convergence culminated with a continent-continent collision (Westaway, 2003), which led to shortening and thickening of the crust in Eastern Anatolia (Şengör et al., 2003), yielding a widespread volcanism (Di Giuseppe et al., 2018). The Tethyan Ocean, originally separating the two

continents, was subducted underneath South-eastern Anatolia and West Iran, (Lustrino et al., 2021). After the collision, a wide orogen developed along the Eurasia-Arabia collision zone (Şengör and Kidd,1979; Dewey et al., 1986) and a large plateau with a relatively flat topography and a slightly thickened crust (40-50 km) developed in Eastern Anatolia (Al-Lazki et al., 2003; Şengör et al., 2003, 2008; Angus et al., 2006). Here a long-lasting subduction-related igneous activity developed. Neogene magmatism in Eastern Anatolia comprises volcanic rocks characterized by complex chronological and geochemical variations (Pearce et al., 1990; Keskin et al., 1998; Keskin, 2003, 2007; Şengör et al., 2008). Here, the oldest activity shows subduction-related geochemical features (Innocenti et al., 1982; Keskin et al., 1998; Keskin, 2003, 2007; Şengör et al., 2008), but alkali-richer lithologies locally occur (Innocenti et al., 1976, 1980; Alici et al., 2001; Alpaslan, 2007; Kurt et al., 2008). Almost all these volcanic activities encompass multiple obsidian products, enlarging the possible supply during ancient times.

The Lake Van area (Eastern Anatolia, Fig. 2b) is of particular interest for the network exchanges because it was connected to prehistoric populations of the Upper Tigris River and into Mesopotamia through pathways and riverine transport (Carter et al., 2013, 2021). The discovery of obsidians tools in Körtik Tepe (Southeastern Anatolia) since the late 11th and early 10th millennium BC coming from the obsidian sources of Bingöl plateau and Nemrut Dağ volcano confirm this hypothesis (Carter et al., 2013). In addition, several obsidian tools, vessels and other artifacts were discovered in the Mesopotamia (Fertile Crescent), Iran, Eastern Türkiye and the whole Middle East, and referred to the Nemrut Dağ volcano as material source area (see e.g., Chataigner et al., 1998; Healey, 2007, 2013, 2021, 2025 and references therein).

Moreover, the occurrence in this area of obsidians characterized by very high concentrations of incompatible elements such as zirconium and rubidium, relatively high levels of compatible elements such as Zn, Mn, and Ti, and a predominantly peraluminous rather than peralkaline affinity, immediately led us to consider the Lake Van area as a possible source for the Tulul artefacts. Same for archaeological obsidian objects found in several locations (see e.g., Chataigner et al., 1998; Frahm, 2012, 2023, 2024, 2025; Healey, 2007, 2013, 2021, 2025 and references therein). Therefore, our interest will be focused on Nemrut Dağ volcano and Bingöl plateau.

2.2 Nemrut Dağ volcano and Bingöl plateau: Obsidian occurrence and outcrops

Nemrut Dağ stratovolcano and Bingöl plateau are located in the Lake Van area of South-eastern Anatolia (Fig. 2b). Geological investigations in the Lake Van area have shown the occurrence of a calc-alkaline volcanism active at least since Lower Miocene, and an alkaline one, beginning around 6 Ma ago (Innocenti et al., 1982). Two different stages of calc-alkaline volcanism can be distinguished (Innocenti et al., 1976). The first one is of high-K type and is represented by large flows and numerous domes. It ended with the eruptions of major ignimbritic flows around 6 Ma. The second stage of activity began with the build-up of major stratovolcanoes. Calc-alkaline volcanic activity is related to subduction of the Arabian plate under the Anatolian-Iranian continental one, whereas the alkaline volcanism is the consequence to the continental collision of the two plates in Upper Miocene which caused the fragmentation and the divergent motion of the Anatolian and Iranian continental mass (Innocenti et al., 1982) up to the formation of the Van microplate (Nouri et al., 2016; Azizi and Tsuboi, 2021).

Volcanism in Van microplate varies from the mildly alkaline (Nemrut Dağ volcano) in the South to the transitional calc-alkaline/mild-alkaline (Bingöl volcanic plateau) in the North-West (Innocenti et al., 1980).

Nemrut Dağ is an active polygenic stratovolcano, with a typical volcanic activity following extensive N-S crustal processes in the Quaternary Age, which experienced historical eruptions (Aydar et al., 2003). Located North of Tatvan, this stratovolcano, culminates at 2935 m, covers an area of about 36 km^2, and with its vast caldera, partially occupied by a lake, near the South-western tip of Lake Van (1648 m above sea level) (Karaoglu et al., 2005), reaches 25 km in diameter.

Since a few decades, an increasing number of studies (Özdemir et al., 2006) concern the geology of the Nemrut Dağ whose eruptive activity can be divided at least in two stages: a pre-caldera and a post-caldera phases. Obsidian is present at every stage of the build-up of the stratovolcano.

In the pre-caldera stage, the oldest obsidian flows occur at the bottom of the caldera wall (75-150 m thick) and at about 8 km north and northwest of the caldera. In the upper part of the caldera wall, above the trachytic and trachy-andesitic lavas (above the oldest obsidian flow) lies another obsidian flow bearing sanidine phenocrysts 1-2 cm in size; this flow constitutes also large outcrops on the southern and eastern flanks and is present in minor quantities on the North-eastern flank.

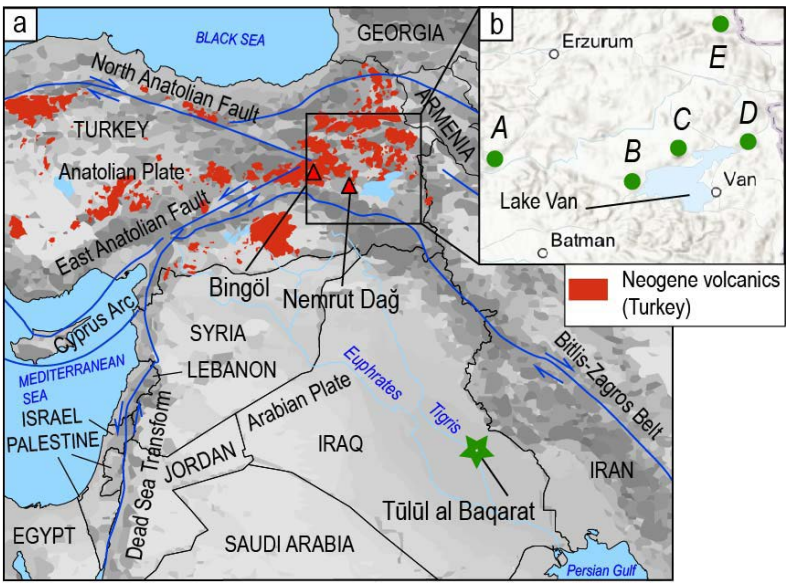

Figure 2. (a) Geological map of the Near East, with reported the Neogene volcanics of the Türkiye (modified after Asan, 2020). Bingöl and Nemrut Dağ volcanoes are indicated with red triangles. Tūlūl al-Baqarat archaeological area is indicated by the green star (central-south Iraq). (b) Detail of the Lake Van area (oriental Türkiye), showing the main regional obsidian areas (Khazaee et al., 2014). Sources: (A) Bingöl, (B) Nemrut Dağ, (C) Suphan Dağ, (D) Meydan Dağ, (E) Sarikamis. Modified after Vaggelli et al. (2025).

In the post-caldera stage, repeated pyroclastic flows were accumulated in the caldera floor, where they formed ponded ignimbrites, accompanied by big, glassy, black obsidian flows, characterized by massive flow banding (Yilmaz et al., 1998). During the last stages vitrophyric rhyolite flows occur along a rift zone to the North of the caldera. Therefore, the obsidian flows, fragmented deposits and chops, outcrop in multiple areas both inside and outside the caldera as well as on its walls (Karaoglu, 2003).

Chataigner et al. (1998) argued that Nemrut Dağ obsidian was the principal source for obsidians in Mesopotamia and that the deposits of Bingöl A had a relatively limited distribution. However, in more recent archaeological literature, Muskara and Konak (2021) as well as Muskara and Ağırsoy (2023) suggest that Bingöl B, Bingöl A and Nemrut Dağ were the principal sources at both Gre Fılla and Kendale Hecala. Despite the amount of data available in the literature listed above, almost no data about the stratigraphy of the obsidian outcrops is available. Furthermore, literature does not provide any information about obsidian emplacement (Robin et al., 2016).

The Bingöl volcanic complex is a basaltic plateau with enormous thickness (up to 1000 m) of almost horizontal flows of extrusive rocks. Numerous streams of the area have eroded deep and narrow valleys in this plateau (Kurum and Baykara, 2020). Its volcanic rocks are products of the volcanic activities occurred in collisional and post collisional – post orogenic stages along the suture zone between the Anatolian and the Eurasian plates. The volcanic suite is made up of calc-alkaline to weakly alkaline basic-intermediate lavas and pyroclastics; mild alkaline and calc-alkaline obsidian varieties also occur: these obsidians are known as “Bingöl A” and “Bingöl B”, respectively (Cauvin et al., 1986).

More in details, the mild alkaline variant of Bingöl-A crops out in a small flow known as Orta Duz and in the secondary epiclastic deposit Cavuslar, dated like the calc-alkaline variant from 4 to 8 Ma by fission tracks (Bigazzi et al., 1997). Further Ar/Ar dating suggests a narrower range since Orta Duz and Cavuslar samples which are dated at 4.2 $\pm$ 0.1 Ma and 4.6 $\pm$ 0.1 Ma, respectively.

Frahm (2012) reports the first representative available dataset of georeferenced Nemrut Dağ and “Bingöl A” obsidians based on electron microprobe analyses of 100 geological obsidian samples provided by G. Rapp who along with T. Ercan participated in an obsidian field survey in the Nemrut region (Bigazzi et al., 1994). According to G. Rapp (Frahm, 2012), eleven obsidian outcrops were identified inside and outside of the Nemrut caldera (Bigazzi et al., 1997) which were geochemically grouped in 6 clusters (Nemrut 1-6) by Frahm, 2012, suggesting the occurrence of rhyolites from calc-alkaline (Nemrut 1) to variably alkaline (Nemrut 2-5), up to the Fe-rich and Al-poor rhyolite variety (Nemrut 6).

Robin et al. (2016) reported a further obsidian outcrop of Nemrut volcano close to Sicaksu and considers this occurrence as the most probable source site for obsidian tools due to the obsidian blocks size and to the well glassy micro-texture devoid of microcrystals or cracks. Frahm (2020), finally, hypothesizes the geochemical similarity between the Nemrut 2 obsidian cluster of Frahm (2012) and the Sicaksu obsidian deposit of Robin et al. (2016). Finally, Frahm (2023, 2025) provides an extensive set of data that significantly enhances to our understanding of the geochemistry of most Turkish obsidians.

3. Material and Methods

3.1 Analitical techniques and methodology

Major and minor elements of the nine obsidian samples (Fig. 3a) were performed by a scanning electron microscope (SEM – JEOL IT-300LV) equipped with an energy dispersive microanalysis system (SDD EDS detector – Aztec Oxford Instruments). To avoid coating, measurements were obtained operating under low vacuum conditions that allow analysis with a non-invasive and non-destructive approach. The possibility of operating in a completely non-invasive way represents a non-negligible incentive to the development of specific analytical protocols for applications to the heritage of cultural and archaeological interest.

The compositional homogeneity of each tool was verified by quartering the sample surface and acquiring X-Ray elemental maps of about 1 mm^2 (total area of 4 mm^2) on each sample.

The operating conditions for each single quartered map were acceleration voltage 30 kV, low vacuum 50 Pa, beam current 5 nA, working distance 10 mm, dwell time 5 ms, 2×10^8 counts.

Each map was acquired avoiding small holes, cracks, scratches, and microlites (Fig. 3b, c, d). The software used for the elemental acquisition is Aztec Oxford Instrument ®, Features package.

From each area (Fig. 3e), the sum spectrum was extracted and then quantified with Oxford Instruments AZtec QuantMap: mean and standard deviation was calculated, item by element. Primary and Secondary Standards used for EDS quant calibration and check are the minerals from Astimex Scientific Limited®53 Minerals Mount.

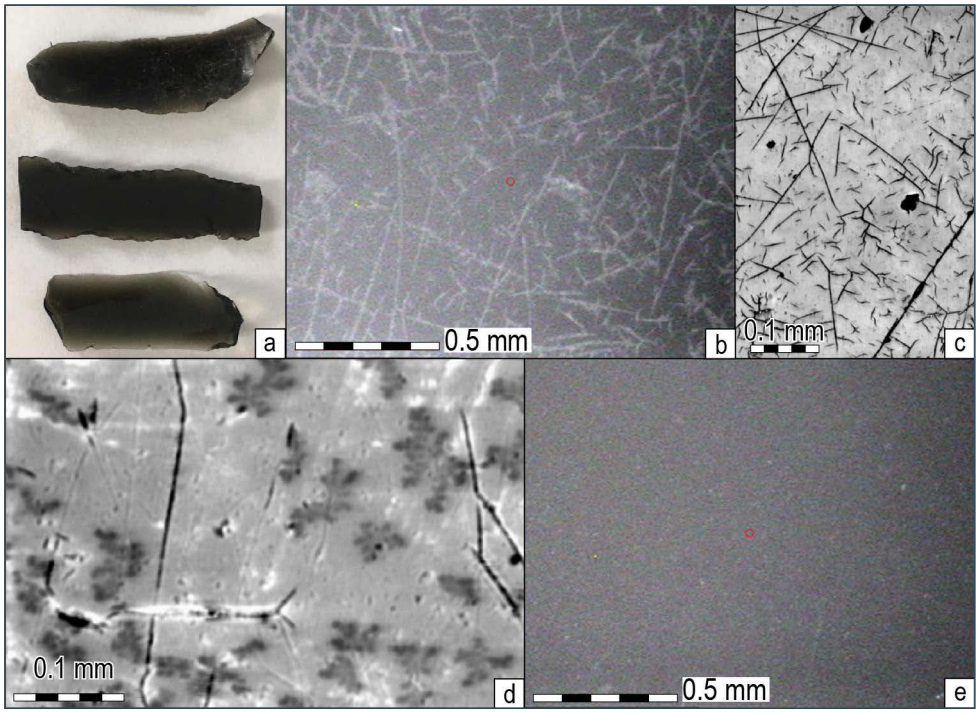

Figure 3. (a) Macroscopic view of three obsidian tools; (b) microphotograph in plane-polarized light; (c,d) back-scattered electron (BSE) images showing surface scratches (c), microlites and devitrified areas (d); (e) plane-polarized light microphotograph of a clean area used for compositional analysis.

The detection and quantification of trace elements was obtained by means of a benchtop EDAX-Eagle micro-fluorescence (micro-XRF). The micro-XRF uses a beam of collimated polychromatic X-rays to produce the characteristic X-rays of the chemical elements in conditions of high analytical sensitivity that allows to measure, always in non-destructive mode, contents lower than 1000 ppm (Vaggelli and Cossio, 2012). The analytical conditions of the micro-XRF were as follows: acceleration voltage 40 kV, beam current 1 mA, counting time 1000 s, XRF beam spot 30 µm. A 250 µm thick aluminium foil was used as primary filter and the correction method "Fundamental Parameter" with internal standards was applied for the quantitative results, using two reference standards for glass materials: NIST610 and NIST612 (more details in Vaggelli et al., 2013).

The trace elements were determined as a profile of ten spot analyses performed along the elongation of the tool being careful to avoid small holes, scratches or non-flat areas as shown by the tool surfaces reported in the pictures by reflected light microscope (Fig. 3b) and by SEM back-scattered electron (BSE) images (Fig. 3c, d).

At first, a geochemical comparison of the obtained results with obsidian sources from the Turkish/Armenian areas, reported in literature, was performed and followed by a Principal Component Analysis (PCA: Covariate matrix; Vaggelli et al., 2025). Finally, a machine learning approach was used for the conclusive attribution of the obsidian tools to their sourcing, and so, to validate the discriminatory capacity of different set of geochemical elements in any archaeometric studies of different laboratories and/or obtained with different analytical techniques

3.2 Machine Learning approach: Decision Trees and Random Forest

Although it is difficult to distinguish Bingöl peralkaline from Nemrut Dağ obsidians, it seems that most of the peralkaline artefacts found in the Near East belong to the Nemrut Dağ source and that the deposits of Bingöl peralkaline had a relatively limited diffusion. Since 9600 BC up to about 6000 BC, Bingöl peralkaline obsidian is present in the basins of the upper Tigris (Çayonu) and upper Euphrates (Cafer) and followed the diffusion of the calc-alkaline variant towards the middle Euphrates not going beyond the oasis El Kowm of the Syrian desert (Cauvin et al., 1991; Gratuze et al., 1993; Chataigner, 1998; Poidevin, 1998; Carter et al., 2013, 2021).

However, a comprehensive geochemical method for distinguishing between Nemrut Dağ and Bingöl A obsidians still needs to be developed and applied. To address this, we have successfully tested this scientific and archaeometric challenge using a machine learning approach based on "Decision Trees" and "Random Forest" models.

A well-known top-down classification algorithm is decision trees (Qinlan, 1986). This algorithm constructs tree-like graphs. Two abstractions are used: the nodes and the branches. Branches simply connect nodes with each other. The nodes make decisions: they can send an instance to another node (termed a child node) that is connected through a branch, or they can return the estimated class of an instance if it is a final node or leaf node. In the root (the first node), all instances are used to determine which is the best attribute for splitting the instances in two subsets assigned to two new child nodes. This process is recursively repeated in each new node until the class of all instances of the subset is unique or until a stopping criterion is reached. The best attribute is determined in each node by evaluating the Information Gain or Gini Index.

A Random Forest (Breiman, 2001) is a meta-classifier (or ensemble) that trains several decision trees on various subsamples of the original dataset and uses averaging to improve the predictive accuracy and control over-fitting. A random forest can assign importance to the different attributes of a data set, and it is also one of the most cited classifiers for the best results, which makes it interesting to study it in this context.

The Random Forest algorithm was applied using geochemical analyses on obsidian sourcing from Frahm (2012) for creating the training data sets. Random forest is an ensemble learning method for classification that operates by constructing a multitude of decision trees (Quinlan, 2014) at training time: the output of the random forest is the class selected by most trees (Breiman, 2001).

The Random Forest calculations were performed by means of Sharp Learning (SharpLearning software package) library, using the default parameters (100 Trees). The returned output includes a list of probabilities (1 for each output class) where the highest value corresponds to the most probable phase.

The algorithm must be trained by associating the input variables (in our case the concentrations of the elements) with the class they belong to. From here on it is possible to enter input variables (concentrations of elements in an unknown sample) to obtain the most probable class: that is, for each available class, we have the probability (0÷1) of belonging (Cossio et al., 2024).

4. Results and Discussions

4.1 Geochemical data of Tūlūl al Baqarat obsidian tools

Table 1 shows the average with relative standard deviation of the performed multiple analyses for major and minor elements, in each individual area. The detected trace elements are mostly "Incompatible" high strength field elements (HFSE: Y, Zr and Nb), in addition to Rb and Zn. Measured as single spot analyses, such elements are reported as average values and relative standard deviation.

The representative chemical compositions suggest that the analysed tools were machined from a natural volcanic glass with high SiO_2 (>70 wt.%) and alkaline ($Na_2O + K_2O$) contents, this latter roughly 10 wt.%, indicating

Table 1. Microchemical analyses of nine obsidian tools (OBS1-9) from Tūlūl al Baqarat. Major and Minor (Mn, Ti and Zr) elements were determined by SEM-EDS detector by Oxford Instruments. Trace elements by µ-XRF by EDAX Instruments Modified after Vaggelli et al. (2025).

Major elements (wt.% oxide)								
Label	SiO_2	Al_2O_3	FeO	MgO	CaO	Na_2O	K_2O	P_2O_5
OBS1	75.40 ± 0.16	11.35 ± 0.17	2.64 ± 0.06	0.03 ± 0.03	0.45 ± 0.20	4.32 ± 0.14	5.83 ± 0.16	0.04 ± 0.02
OBS2	75.17 ± 0.13	11.37 ± 0.08	2.70 ± 0.06	0.36 ± 0.20	0.62 ± 0.19	5.11 ± 0.06	4.56 ± 0.03	0.07 ± 0.02
OBS3	75.52 ± 0.10	11.57 ± 0.05	2.67 ± 0.08	0.60 ± 0.16	0.48 ± 0.03	4.94 ± 0.19	4.48 ± 0.06	0.05 ± 0.01
OBS4	75.47 ± 0.45	11.54 ± 0.20	2.66 ± 0.19	0.11 ± 0.06	0.33 ± 0.05	5.05 ± 0.02	4.63 ± 0.09	0.06 ± 0.02
OBS5	76.08 ± 0.22	11.47 ± 0.03	2.70 ± 0.07	0.05 ± 0.05	0.25 ± 0.05	4.26 ± 0.16	4.82 ± 0.31	0.03 ± 0.03
OBS6	75.53 ± 0.19	11.38 ± 0.05	2.66 ± 0.03	0.18 ± 0.04	0.24 ± 0.05	5.05 ± 0.28	4.50 ± 0.09	0.07 ± 0.02
OBS7	75.44 ± 0.22	11.34 ± 0.07	2.77 ± 0.04	0.39 ± 0.07	0.48 ± 0.10	5.19 ± 0.18	4.63 ± 0.07	0.11 ± 0.03
OBS8	75.71 ± 0.06	11.41 ± 0.03	2.44 ± 0.06	0.01 ± 0.02	0.22 ± 0.02	5.46 ± 0.07	4.40 ± 0.04	0.08 ± 0.02
OBS9	75.24 ± 0.04	11.42 ± 0.07	2.48 ± 0.03	0.21 ± 0.02	0.34 ± 0.02	5.60 ± 0.08	4.28 ± 0.05	0.09 ± 0.04

Minor/Trace elements (ppm)							
Label	Mn	Ti	Zn	Rb	Zr	Y	Nb
OBS1	415 ± 69	839 ± 36	231 ± 8	286 ± 7	1414 ± 22	155 ± 7	73 ± 5
OBS2	438 ± 73	1019 ± 44	240 ± 29	277 ± 5	1408 ± 15	156 ± 5	77 ± 4
OBS3	453 ± 75	899 ± 39	235 ± 22	259 ± 15	1240 ±82	148 ± 15	70 ± 8
OBS4	394 ± 65	779 ± 33	235 ± 10	274 ± 40	1415 ± 16	162 ± 5	80 ± 5
OBS5	439 ± 73	959 ± 41	231 ± 25	286 ± 46	1370 ± 101	143 ± 8	219 ± 2
OBS6	380 ± 63	905 ± 39	187 ± 5	250 ± 9	1336 ± 12	139 ± 2	82 ± 3
OBS7	374 ± 62	785± 34	201 ± 18	239 ± 9	1251 ± 61	145 ± 14	73 ± 6
OBS8	410 ± 68	815 ± 35	219 ± 5	265 ± 16	1398 ± 35	155 ± 8	86 ± 13
OBS9	445 ± 74	795 ± 34	218 ± 6	256 ± 2	1426 ± 6	161 ± 4	86 ± 2
Data reported as mean value ± standard deviation. Sr < bdl (i.e. <50 ppm).							

a rhyolitic composition with low alumina (Al_2O_3 around 11 wt.%) and calcium (CaO <1 wt.%; Vaggelli et al., 2020) contents. As for trace elements, the very high content in Zr (>1000 ppm), Rb (200-300 ppm), Y (140-150 ppm), Nb (50-80 ppm) and Zn (150-200 ppm; Table 1) are peculiar features reflecting acid volcanic rocks occurring in Eastern Anatolia (Innocenti et al., 1982; Di Giuseppe et al., 2017).

4.2 Geochemical comparison of Tūlūl al Baqarat samples with obsidian sources

The data produced are firstly compared with obsidian sources from the most widespread obsidian-bearing Turkish volcanic areas reported in literature (Keller and Seifried, 1991; Khademi Nadooshan et al., 2013; Khazaee et al., 2014; Darabi and Glascock, 2013). However, for simplicity and clarity we have restricted our consideration to the most significant and analytically best constrained elements as Zr and Rb, which have a preliminary discriminatory capacity in this large volcanic contest and because their high values are clearly different from most obsidian sources of calc-alkaline affinity (Di Giuseppe et al., 2018) excluding any Armenian, western Anatolia or Cappadocia potential obsidian sources (Fig. 4a).

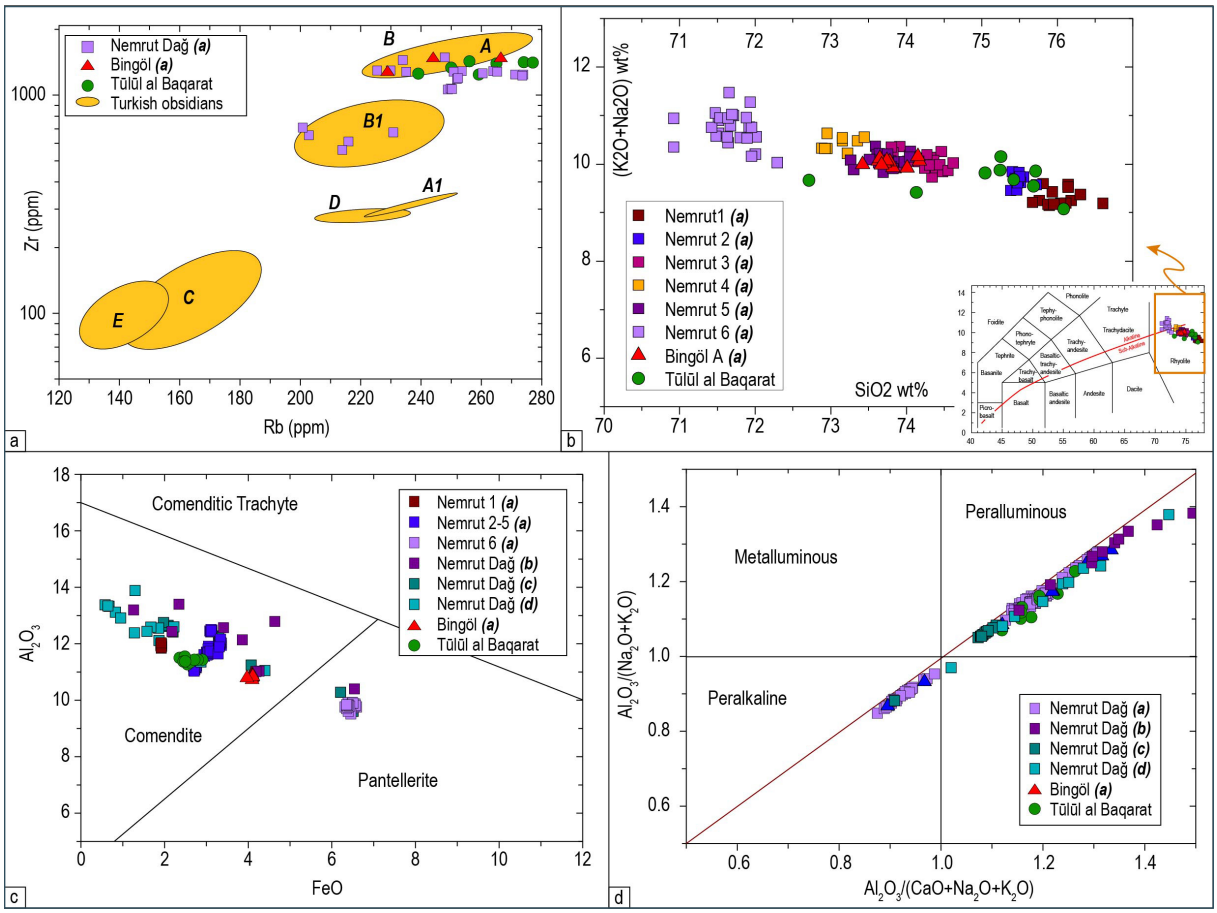

Figure 4. (a) Rb vs Zr diagram. Orange fields refers to Turkish obsidians (A: Bingöl-A; A1: Bingöl-B; B: Nemrut Dağ; B1: Nemrut Dağ; C: Suphan Dağ; D: Meydan Dağ; E: Sarikamis) in Lake Van volcanic area. Modified after Khazaee et al. (2014). A selection of georeferenced obsidian samples from Nemrut Dağ and Bingöl (Frahm, 2012) are plotted with Tūlūl al-Baqarat tools, for comparison. (b) Detail of the diagram Total-Alkali vs Silica (TAS, after LeBas et al., 1986) classification diagram showing the composition of the nine Tulūl al-Baqarat obsidians. (c) Classification diagram of trachytes and Rhyolites of comenditic and pantelleritic types based on Al_2O_3 and FeO contents (MacDonald, 1974). (d) A/NK vs. A/CNK diagram showing peralkaline to peraluminous nature of the Obsidians from Nemrut Dağ and Bingöl sources. Reference data in each graph: (*a*) Frahm (2012); (*b*) Keller and Seifried (1991); (*c*) Sumita and Schmincke (2013); (*d*) Schmincke and Sumita (2014).

Among the possible source areas for obsidian tools found in the site of the Tūlūl al Baqarat archaeological area, only the mild alkaline/transitional obsidians (Fig. 4b) from Nemrut Dağ and Bingöl A (Lake Van area, South-eastern Türkiye; Fig. 2b) show values in Zr > 1000 ppm and Rb > 200 ppm, similarly to Tūlūl al Baqarat obsidian tools (Fig. 4a). Bingöl B and Nemrut 1 (Frahm, 2012) clusters can also be excluded according to the relatively low Zr content (<500 ppm).

Therefore, an accurate comparison with obsidians erupted from Nemrut Dağ stratovolcano and Bingöl plateau must be performed because these two peralkaline/peraluminous sources have a very similar geochemical imprint. Following this assumption and in agreement with literature studies on Bingöl A and Nemrut obsidians, a set of bivariate and three-dimensional diagram have been performed using the available data sets from literature (Keller and Seyfried, 1999; Frahm, 2012; Sumita and Shmincke, 2013 – Mainz georef rock; Carter et al., 2013; Shmincke and Sumita, 2014; Robin et al., 2016).

4.3 Geochemical comparison of Tūlūl al Baqarat tools with obsidian sources from Nemrut Dağ and Bingöl

In the classification diagram Al_2O_3-FeO for rhyolites (Fig. 4c; Mc Donald, 1974) obsidian tools can be classified as Comendite, with peralluminous affinity (Fig. 4c) as well as Bingöl A and most Nemrut Dağ obsidians (Frahm, 2012; Carter et al., 2013, Keller and Seyfried, 1991, Shmincke and Sumita, 2014; Sumita and Shmincke, 2013; Mainz georef rock). The separate set of Nemrut obsidians with pantellerite composition and peralkaline affinity (Fig. 4c) corresponds to "Nemrut 6" cluster of Fahm (2012), which is also characterized by Fe-rich and Al-poor values (FeO >6 wt.% and Al_2O_3 <10wt%; Fig. 4a). The peralkaline or peraluminous nature of Nemrut Dağ obsidians (Fig. 4d) indicate the post-caldera or the pre-caldera volcanic flows, respectively (Chataigner et al., 1998).

Finally, in the SiO2 and Alkali diagram (Fig. 4b), the negative trend between SiO_2 and Alkali display and support the geochemical grouping of Frahm (2012) classes, in agreement with Ercan outcrops. Therefore, hereafter

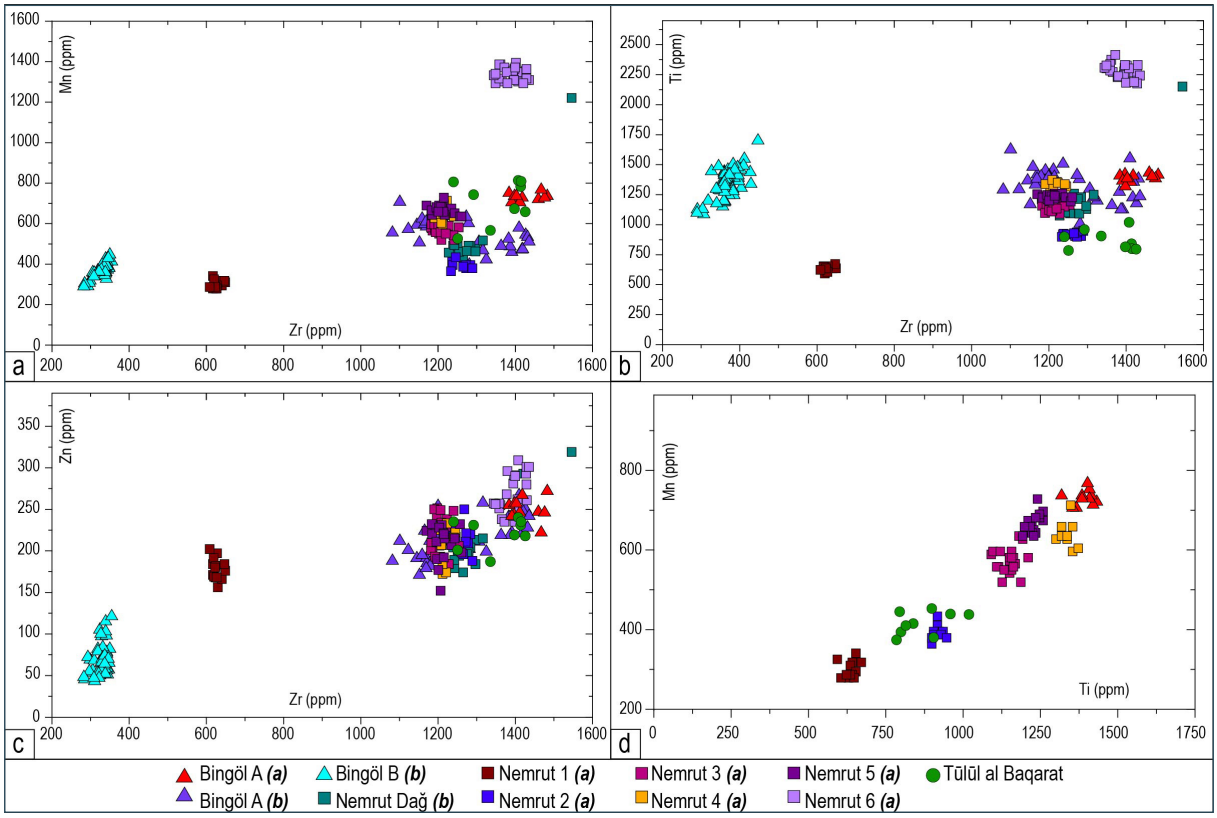

Figure 5. (a, b, c) Zr vs Mn, vs Zn and vs Ti diagrams and (d) Ti vs Mn diagram for Tūlūl al Baqarat tools compared with obsidian sources from Nemrut Dağ and Bingöl. Data from (a) Frahm (2012) and (b) Carter et al. (2013).

the geochemical comparison will be carried out exclusively with Frahm (2012) data. Moreover, it suggests the selection of Si, Na and K as rather discriminative major elements for the machine learning approach.

In the diagrams of Fig. 5 the selected trace element pairs such as Zr vs Zn, Mn, Rb, Ti, show a scarce discriminating capacity, in disagreement with Khademi Nadooshan et al. (2013) and Khazaee et al. (2014). Indeed, in the diagram Zr vs Zn and Mn "compatible" elements, a clear separation between Bingöl-B, Nemrut 1 and Nemrut 6 clusters is shown but not between Nemrut 2-5, Bingöl-A and Tūlūl al Baqarat obsidians. Almost the same, if Zr is plotted vs "incompatible" trace elements as Rb and Ti: an indistinct field of data gathers Nemrut, Bingöl-A and Tūlūl al Baqarat obsidians (Fig. 4a and 5b).

Only in the diagram Mn – Ti (Fig. 5b) an interesting grouping is shown, together with a discrete discriminative capacity of these two elements to separate Frahm (2012) clusters, and an overlap of Tulul al Baqarat tools with Nemrut 2 group. Therefore, it seems useful select these two elements in addition to Zr and Zn, which characterise the geodynamic environment in Lake Van area (South-eastern Anatolia), as good element for the following machine learning investigation. Three-dimensional diagrams have been performed both using the trace/minor elements as Mn-Ti-Zr and the trace/major elements as Zr-FeO-Zn, whose values are peculiar contents in the obsidian tools.

Despite, as shown in Figs. 6a and 6b, no attribution of the obsidian tools can be considered exhaustive; a good separation between Nemrut 1 and Nemrut 6 cluster is again observable as well as a grouping from Nemrut 2 up to Nemrtut5, but Tūlūl al Baqarat samples fall within Nemrut 2-5 and Bingöl-A clusters. Because no final exhaustive and undoubted information was obtained by a detailed geochemical comparison, an innovative attempt was performed applying a machine learning model based on literature data from Frahm (2012) as training dataset. Indeed, Frahm (2012) provides the best representative available dataset, based on electron microprobe analyses, containing 100 georeferenced Nemrut Dağ and Bingöl obsidians, grouped in definite classes (six clusters named Nemrut 1-6 besides Bingöl A) and occurring in different outcrops with similar geochemical imprints.

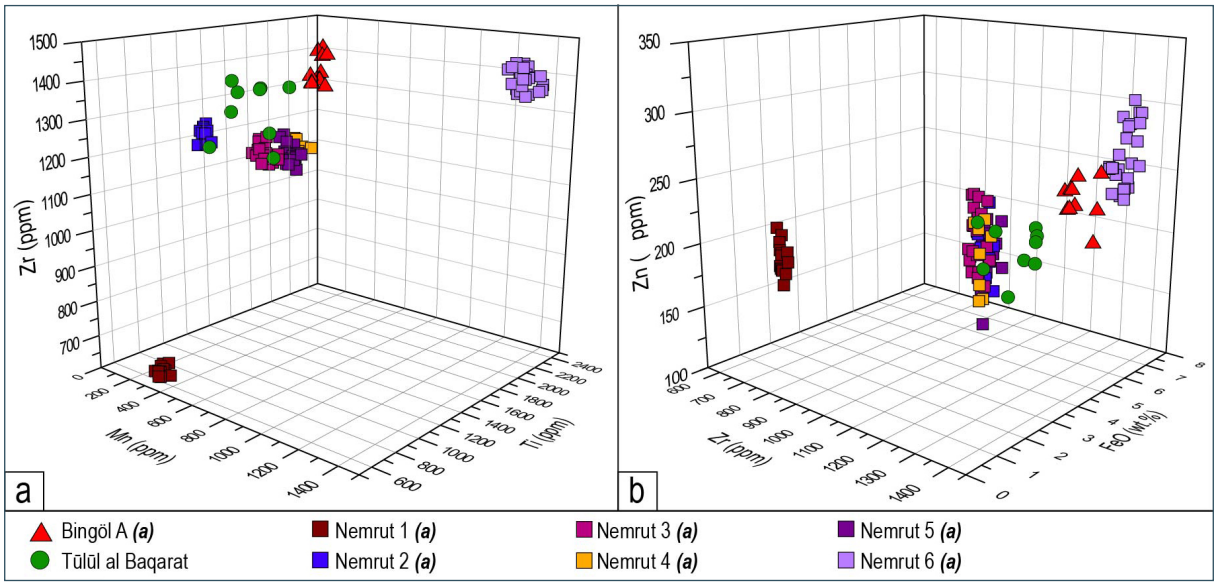

Figure 6. (a) Zr-FeO-Zn and (b) Mn-Ti-Zr three-dimensional plots for Tūlūl al Baqarat tools compared to Nemrut and Bingöl obsidian sources from (a) Frahm (2012).

4.4 The Machine Learning approach

Given the good separation between the Frahm (2012) clusters as tested with a Principal Componet Analysis (PCA) analysis reported in Vaggelli et al. (2025) it is possible to proceed with machine learning model, based on "The Random Forest" algorithm (Quinlan, 2014).

The Random Forest algorithm was applied using geochemical analyses on obsidian sourcing from Frahm (2012) for creating the training dataset, using Nemrut 1-6 and Bingöl-A groups as classes. The returned output includes a list of probabilities (1 for each output class) where the highest value corresponds to the most probable phase.

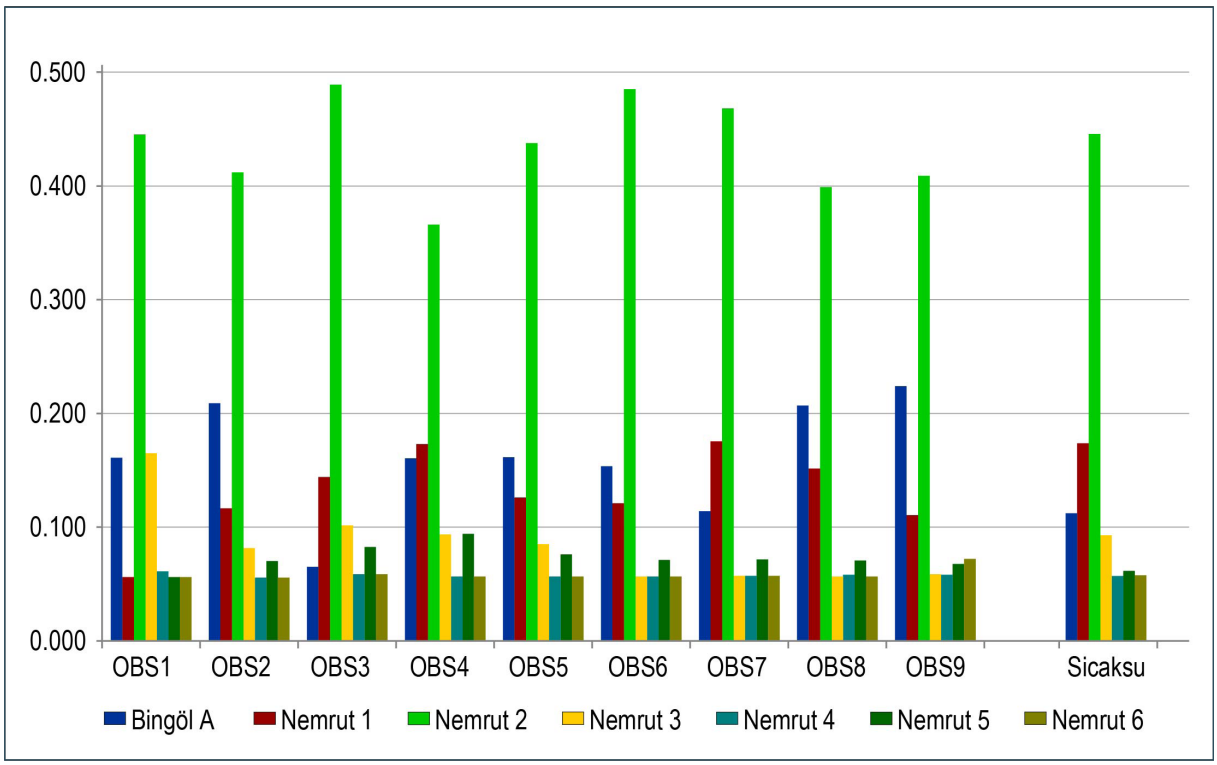

Figure 7. Random Forest (RF) averaged Decision Probability for Tūlūl al Baqarat obsidian tools (OBS1-9). The mean chemical composition of Sicaksu obsidian samples from Robin et al., 2016 are also tested and displayed (see text).

The algorithm must be trained by associating the input variables (in our case the concentrations of the elements) with the class they belong to. From here on it is possible to enter input variables (concentrations of elements in an unknown sample) to obtain the most probable class (0÷1 of belonging probability).

The chemical elements selected for the machine learning approach consist of five major elements (Si, Al, Fe, Na, and K) and four minor/trace elements (Ti, Mn, Zr, and Zn), which were identified as the most discriminative elements in geochemical comparisons and PCA analysis (Vaggelli et al., 2025).

In Fig. 7 is reported the histogram of provenance probability for each obsidian tool (Table 2), calculated as average value from major and minor/trace elements probability of belonging. The diagram displays a coherent unique provenance for the raw material of the nine obsidian tools from Nemrut 2 cluster which corresponds to an outcrop inside the caldera, likely emplaced during the pre-caldera stage of Nemrut volcano. According to Frahm (2020), Nemrut 2 cluster is geochemically compatible to Sicaksu obsidian deposit described by Robin et al. (2016), which crops out North-West the Nemrut Caldera. Therefore, the geochemical mean analysis of Sicaksu georeferenced obsidian reported as averaged value by Frahm (2020) have been tested with the same algorithm developed for Tūlūl al Baqarat.

The result reported in Fig. 7 strongly support the geochemical affinity and thus a potential volcanological link between the Sicaksu obsidian and the Nemrut 2 source. The calculated average probability of the Sicaksu obsidian belonging to Nemrut 2 is the highest among the compared sources and closely aligns with that of the Tūlūl al Baqarat tools (Table 2).

This suggests a possible cogenetic origin and emplacement for both alkaline peraluminous obsidian deposits, identified at Sicaksu (Robin et al., 2016) and within the Nemrut caldera (Cluster Nemrut 2 of Frahm, 2012, 2020).

This hypothesis may confirm the probable sourcing of the studied obsidians from the Stratovolcano Nemrut Dağ, and more precisely from the peralkaline/peraluminous obsidians occurring in an outcrop inside caldera (Nemrut 2 of Frahm, 2012, 2020). These obsidians are geochemically comparable to the obsidians in Sicaksu outcrop described by Robin et al. (2016), which further confirm the possible obsidian source.

This interpretation opens new questions on the trade route (several hundreads of km) from the source to the archaeological site of obsidian tools discovery. Oddone et al. (2003) suggest that other factors besides geographical position influenced obsidian circulation. even assuming their transport to the site of discovery.

This archaeometric study suggests therefore the existence of extensive interaction networks through the main waterways of the region (e.g., the Tigris River) between populations of Southeastern Anatolia and the Southern Near East during the 4th millennium BC.

Moreover, the results offer valuable insights for volcanological research in the Lake Van region of eastern Türkiye. Indeed, the strong "calculated" geochemical similarities, between the Nemrut Cluster 2 and Sicaksu obsidians suggest a close connection between the two deposits, potentially challenging the previous identification of the origin of tools from Nemrut 2. This raises intriguing volcanological implications for reconstructing the volcanic activity of the Nemrut Dağ stratovolcano and underline the value of applying machine learning approaches to volcanological and provenance studies.

Table 2. Random Forest mean (Major & Minor /Trace elements) decision probability. OBS = Obsidian Tool. Sicaksu = Sicaksu Obsidian (mean composition from Robin et al., 2016 reported in Frahm, 2022).

RF mean	Bingöl A	Nemrut 1	Nemrut 2	Nemrut 3	Nemrut 4	Nemrut 5	Nemrut 6
OBS1	0.161	0.056	***0.445***	0.165	0.061	0.056	0.056
OBS2	0.209	0.117	***0.412***	0.082	0.056	0.070	0.056
OBS3	0.065	0.144	***0.489***	0.102	0.059	0.083	0.059
OBS4	0.161	0.173	***0.366***	0.094	0.057	0.094	0.057
OBS5	0.162	0.126	***0.438***	0.085	0.057	0.076	0.057
OBS6	0.154	0.121	***0.485***	0.057	0.057	0.071	0.057
OBS7	0.114	0.176	***0.468***	0.057	0.057	0.072	0.057
OBS8	0.207	0.152	***0.399***	0.057	0.058	0.071	0.057
OBS9	0.224	0.111	***0.409***	0.059	0.058	0.068	0.072
Sicaksu	0.111	0.172	***0.446***	0.091	0.056	0.060	0.056

5. Conclusions

The obsidian tools found in Tūlūl al Baqarat settlement show a doubtless composition very different from both Armenian and central or western Turkish obsidians, resulting comparable to the volcanic glasses erupted in Quaternary time from the Nemrut Volcano in South-eastern Türkiye. More in details, the obsidian tools result geochemically comparable to Nemrut Dağ mild alkaline rhyolitic obsidians from pre-caldera eruptions, now cropping out inside the caldera and in Sicaksu outcrop, suggesting a far well distance provenance and sourcing with respect to the settlement, and supporting the extraordinary influence of the Tigris River in the Near East.

It is worthy to note that pairs of minor and trace elements (e.g., Mn Vs Ti, Zr vs Zn, and Zr vs Mn) generally exhibit a satisfying discriminating capacity for most Anatolian obsidian sources. However, for the accurate and comprehensive distinction of similar petrogenetic sources, such as Nemrut and Bingöl obsidians in southeastern Anatolia, a machine learning approach is required. Indeed, Machine learning is definitively able to reliably discriminate between very similar obsidian sources, even when analyzed with different methods or in different laboratories.

The data obtained from this archaeometric study through non-invasive and non-destructive geochemical analyses and through a machine learning approach suggest that the Nemrut Dağ obsidian deposits were very important

as obsidian source to produce tools and artefacts by prehistoric populations across the Near East. It indicates therefore a network of trade and exchange amongst populations of South-eastern Anatolia and the South Near East during the 4th millennium and inferencing paramount information for any archaeological studies on prehistoric settlements.

The chemical compositions of obsidian artefacts can be, therefore, used to reconstruct obsidian exchange networks involving Near East settlements and we can assert that obsidian tool production was not only for local or regional production but was part of a larger regional trade network in obsidian tools (Kalidi et al., 2013). However, it seems that the deposits of Bingöl-A peralkaline/peralumionous had a relatively limited diffusion occurring only in the basins of the upper Tigris and upper Euphrates and followed the diffusion of the calc-alkaline variant (Bingöl-B) towards the middle Euphrates (Gratuze et al., 1993).

On the other hand, the sourcing of the studied obsidians is to be found in the Nemrut Dağ stratovolcano – in the Turkish region of Lake Van – and more precisely from the peraluminous obsidians occurring in an outcrop inside caldera (Cluster Nemrut 2 of Frahm, 2012). However, the significant geochemical similarities observed between the obsidians from Nemrut Cluster 2 and those from Sicaksu indicate a potentially close relationship between these two deposits. This correlation renews and updates previous conclusions regarding the source of the lithic tools identified as originating from Nemrut 2. Such findings open new ways in the field of volcanology, as they suggest the need a revised understanding of the volcanic processes involved in the formation of the Nemrut Dağ stratovolcano. Given these similarities, it may now be plausible to hypothesize a cogenetic origin for the obsidian flows from Nemrut 2 and Sicaksu, implying that they could have been produced by the same (or closely related) volcanic events. This hypothesis would carry significant implications for both the geological history of the region and the archaeological interpretation of obsidian sourcing in the area.

Therefore, this archaeometric study provides also interesting inferences for the volcanological studies in the Turkish region of Lake Van. The displayed robust and definite grouping of obsidian clusters according to Ercan outcrops (Frahm, 2012) and Robin et al. (2016) suggest a volcanic correlation among outcrops, possibly related to different eruption episodes with rhyolitic flows. Indeed, despite the amount of data available in the literature this one does not provide almost any conclusive data concerning the stratigraphy of most obsidian outcrops (Robin et al., 2016) and about obsidian emplacement and magmatic evolution.

Concerning the form in which these raw materials were procured it is more likely that this obsidian was accessed directly, being decorticated at source as a means of both testing raw material quality and diminishing transport weight (Carter et al., 2020). As for the question of how the obsidian was moved to Tūlūl al Baqarat, the sole means of transport was by foot with the domestication of pack animals or on boat. Given the anthropic occupation was very close to Tigris River and extremely far away from the original source, it seems more likely the use of river transportation or a combination of both.

Acknowledgements. CNR-IGG, Dipartimento di Scienze della Terra of Turin University and the interdepartmental Centre "G. Scansetti" (University of Turin) are thanked for sharing laboratories. Special thanks to Mainz Georef Rock for making the dataset available for this study. Financial support was provided by CNR-IGG Torino and by University of Turin through the Dipartimento di Scienze della Terra.

References

Alıcı, P., A. Temel, A. Gourgaud, P. Vidal et al. (2001). Quaternary tholeiitic to alkaline volcanism in the Karasu Valley, Dead Sea Rift Zone, Southeast Turkey: Sr-Nd-Pb-O isotopic and trace-element approaches to crust-mantle interaction, Int. Geol. Rev., 43, 120-138, doi:10.1080/00206810109465004.

Al-Lazki, A. I., D. Seber, E. Sandvol, N. Türkelli et al. (2003). Tomographic Pn velocity and anisotropy structure beneath the Anatolian plateau (eastern Turkey) and surrounding regions, Geophys. Res. Lett., 30, 8043, doi:10.1029/2003GL017391.

Alpaslan, M. (2007). Early to middle Miocene intra-continental basaltic volcanism in the northern part of the Arabian plate, SE Anatolia, Turkey: Geochemistry and petrogenesis, Geol. Mag., 144, 5, 867-882, doi:10.1017/S0016756807003524.

Angus, D. A., D. C. Wilson, E. Sandvol and J. F. Ni (2006). Lithospheric structure of the Arabian and Eurasian collision zone in Eastern Turkey from S-wave receiver functions, Geophys. J. Int., 166, 1335-1346.

Asan, K. (2020). Whole-Rock Elemental and Sr-Nd Isotope Geochemistry and Petrogenesis of the Miocene Elmada Volcanic Complex, Central Anatolia (Ankara, Turkey), Geosciences, 10, 348. doi:10.3390/geosciences10090348.

Azizi, H. and M. Tsuboi (2021). The Van microplate: A new microcontinent at the junction of Iran, Turkey and Armenia, Front. Earth Sci., 8, doi:10.3389/feart.2020.574385.

Aydar, E., A. Gourgaud, I. Ulusoy, F. Digonnet et al. (2003). Morphological analyses of active Mount Nemrut stratovolcano, eastern Turkey: evidence and possible impact areas of future eruption, J. Volcanol. Geotherm. Res., 123, 301-312, doi:10.1016/S0377-0273(03)00002-7.

Bahar, A. (2020). Statues and votive vessels from Tulūl al-Baqarāt, Z. Assyriol., 110, 2, 218-241, doi:10.1515/za-2020-0022.

Bahar, A. (2022). Sumerian and Akkadian Stelae from Tūlūl al-Baqarāt, Rev. Assyriol. Archéol. Orient., 116, 31-41, doi:10.3917/assy.116.0031.

Bigazzi, G., Z. Yeğingil, T. Ercan, M. Oddone et al. (1994). Provenance studies of prehistoric artifacts in Eastern Anatolian: interdisciplinary research results, Mineral. Petrogr. Acta, 37, 17-36.

Bigazzi, G., Z. Yeğingil, T. Ercan, M. Oddone et al. (1997). Age determination of obsidian bearing volcanics in Eastern Anatolia using the fission track dating method, Geol. Bull. Turkey, 40, 2, 57-72.

Breiman, L. (2001). Random Forests, Mach. Learn., 45, 5-32.

Carter, T., S. Grant, M. Kartal, A. Coşkun et al. (2013). Networks and Neolithisation: sourcing obsidian from Körtik Tepe (SE Anatolia), J. Archaeol. Sci., 40,1, 556-569.

Carter, T., K. Campeau and K. Streit (2020). Transregional perspectives: characterizing obsidian consumption at Early Chalcolithic Ein el-Jarba (N. Israel), J. Field Archaeol., 45, 1-21, doi:10.1080/00934690.2020.1717857.

Carter, T., R. Moir, T. Wong, K. Campeau et al. (2021), 'Hunter-fisher-gatherer river transportation: Insights from sourcing the obsidian of Hasankeyf Höyük, a Pre-Pottery Neolithic A village on the Upper Tigris (SE Turkey)', Quaternary Int., 574: 27-42. doi:10.1016/j.quaint.2020.09.045.

Cauvin, M. C., N. Balkan, Y. Besnus and F. Şaroğlu (1986). Origine de l'obsidienne de Cafer Höyük (Turquie): Premiers résultats, Paléorient, 12, 2, 89-97.

Cauvin, M. C., Y. Besnus, J. Tripier and R. Montigny (1991). Nouvelles analyses d'obsidiennes du Proche-Orient: modèle de géochimie des magmas utilisé pour la recherche archéologique, Paléorient, 17, 2, 5-20, doi:10.3406/paleo.1991.4550.

Chataigner, C., J. L. Poidevin and N. O. Arnaud (1998). Turkish occurrences of obsidian and use by prehistoric peoples in the Near East from 14,000 to 6000 BP, J. Volcanol. Geotherm. Res., 85, 1-4, 517-537, doi:10.1016/S0377-0273(98)00069-9.

Cossio, R., S. Ghignone, A. Borghi, A. Corno et al. (2024). A supervised machine learning procedure for EPMA classification and plotting of mineral groups, Appl. Comput. Geosci., 23, 100186, doi:10.1016/j.acags.2024.100186.

Crisci, G. M., R. De Rosa, S. Esperança, R. Mazzuoli et al. (1991). Temporal evolution of a three component system: the island of Lipari (Aeolian Arc, southern Italy), Bull. Volcanol., 53, 3, 207-221.

Darabi, H. and M. D. Glascock (2013). The source of obsidian artefacts found at East Chia Sabz, Western Iran, J. Archaeol. Sci., 40, 10, 3804-3809, doi:10.1016/j.jas.2013.04.022.

Dewey, F. J., M. R. Hempton, W. S. F. Kidd, F. Şaroğlu et al. (1986). Shortening of continental lithosphere: the neotectonics of Eastern Anatolia – a young collision zone, in: Coward, M. P., Ries, A. C. (Eds.), Collision Tectonics, Geol. Soc. London, Spec. Publ., 19, 1-36.

Di Giuseppe, P., S. Agostini, M. Lustrino, Ö. Karaoğlu et al. (2017). Transition from compression to strike-slip tectonics revealed by Miocene-Pleistocene volcanism West of the Karlıova Triple Junction (East Anatolia), J. Petrol., 58, 10, 2055-2087, doi:10.1093/petrology/egx082.

Di Giuseppe, P., S. Agostini, P. Manetti, M. Y. Savaşçın et al. (2018). Sub-lithospheric origin of Na-alkaline and calc-alkaline magmas in a post-collisional tectonic regime: Sr-Nd-Pb isotopes in recent monogenetic volcanism of Cappadocia, Central Turkey, Lithos, 316-317, 304-322, doi:10.1016/j.lithos.2018.07.018.

Donato, P., L. Barba, R. De Rosa, G. Niceforo et al. (2018). Green, grey and black: A comparative study of Sierra de las Navajas (Mexico) and Lipari (Italy) obsidians, Quatern. Int., 467, 369-390.

Frahm, E. (2012). Distinguishing Nemrut Dağ and Bingöl A obsidians: geochemical and landscape differences and the archaeological implications, J. Archaeol. Sci., 39, 1436-1444, doi:10.1016/j.jas.2011.12.038.

Frahm, E. (2020). Variation in Nemrut Dağ obsidian at Pre-Pottery Neolithic to Late Bronze Age sites (or: all that's Nemrut Dağ obsidian isn't the Sıcaksu source), J. Archaeol. Sci.: Rep., 32, 102438, doi:10.1016/j.jasrep.2020.102438.

Frahm, E. and C. M. Carolus (2022). Identifying the origins of obsidian artifacts in the Deh Luran Plain (Southwestern Iran) highlights community connections in the Neolithic Zagros, Proc. Natl. Acad. Sci. U.S.A., 119, 43, e2109321119, doi:10.1073/pnas.2109321119.

Frahm, E. (2023). The obsidian sources of eastern Turkey and the Caucasus: Geochemistry, geology, and geochronology. J. Archaeol. Sci. Rep. 49, 104011, doi:10.1016/j.jasrep.2023.104011.

Frahm, E. (2024). Reassessing the origins of Near Eastern obsidian vessels: Not as simple as "Central Anatolia", J. Archaeol. Sci. Rep., 58, 104731, doi:10.1016/j.jasrep.2024.104731.

Frahm, E. (2025). Archaeological obsidian sourcing: Looking from the first 60 years to the next, J. Arch. Sci., 177, 106200, doi:10.1016/j.jas.2025.106200

Gratuze, B., J. Barrandon, K. Al Isa and M. C. Cauvin (1993). Non-destructive analysis of obsidian artefacts using nuclear techniques: investigation of provenance of Near Eastern artefacts, Archaeometry, 35, 11-21, doi:10.1111/j.1475-4754.1993.tb01020.x.

Healey, E. (2007). Obsidian as an indicator of inter-regional contacts and exchange: three case-studies from the Halaf period. Anatolian Studies, 57,171-189, doi:10.1017/S0066154600008590.

Healey, E. (2013). Exotic, aesthetic and powerful? The non-tool use of obsidian in the later Neolithic of the Near East. In: Nieuwenhiuyse, O.P., Bernbeck, R., Akkermans, P.M. M.G., Rogash, J. (Eds.), Interpreting the Late Neolithic of Upper Mesopotamia. Brepols, Turnhout, Belgium, 251-266.

Healey, E. (2021). Not only a tool-stone: Other ways of using obsidian in the Near East, J. Lithic Studies, 8, 3, 25-83.

Healey, E. (2025). Obsidian Vessels in the Prehistoric and Early Historic Near East. Oxbow Books, 160.

Innocenti, F., R. Mazzuoli, G. Pasquaré, F. Radicati di Brozolo et al. (1976). Evolution of volcanism in the area of interaction between the Arabian, Anatolian and Iranian plates, Lake Van, Eastern Turkey, J. Volcanol. Geotherm. Res., 1, 103-112, doi:10.1016/0377-0273(76)90001-9.

Innocenti, F., R. Mazzuoli, G. Pasquarè, C. Serri et al. (1980). Geology of the volcanic area North of Lake Van (Turkey), Geol. Rundsch., 69, 292-322, doi:10.1007/BF01869038.

Innocenti, F., R. Mazzuoli, G. Pasquarè, F. Radicati di Brozolo et al. (1982). Tertiary and Quaternary volcanism of the Erzurum-Kars area (Eastern Turkey): geochronological data and geodynamic evolution, J. Volcanol. Geotherm. Res., 13, 3, 223-240, doi:10.1016/0377-0273(82)90052-X.

Khademi Nadooshan, F., A. Abedi, M. D. Glascock and N. Eskandari (2013). Provenance of prehistoric obsidian artefacts from Kul Tepe, north-western Iran using X-ray fluorescence (XRF) analysis, J. Archaeol. Sci., 40, 1956-1965, doi:10.1016/j.jas.2012.12.032.

Khazaee, M., M. D. Glascock, P. Masjedi, F. Khademi Nadooshan et al. (2014). Sourcing the obsidian of prehistoric tools found in western Iran to south-eastern Turkey: a case study for the sites of eastern Chia Sabz and Chogha Ahovan, Anatol. Stud., 64, 23-31, doi:10.1017/S0066154614000039.

Karaoğlu, Ö. (2003). Nemrut Kalderası Kuzeyi'nin Jeolojisi Mineralojisi ve Petrografisi, M.Sc. Thesis, Yüzüncü Yıl Univ., Turkey.

Karaoğlu, Ö., Y. Özdemir, A. Ü. Tolluoğlu, M. Karabıyıkoğlu et al. (2005). Stratigraphy of the volcanic products around Nemrut Caldera: implications for reconstruction of the caldera formation, Turk. J. Earth Sci., 14, 123-143.

Keller, J. and C. Seifried (1991). The present status of obsidian source identification in Anatolia and the Near East, Volcanol. Archaeol., PACT, 25, 57-87.

Keskin, M. (2003). Magma generation by slab steepening and breakoff beneath a subduction-accretion complex: An alternative model for collision-related volcanism in Eastern Anatolia, Turkey, Geophys. Res. Lett., 30, 8046, doi:10.1029/2003GL018019.

Keskin, M. (2007). Eastern Anatolia: A hotspot in a collision zone without a mantle plume, in: Foulger, G. R., Jurdy, D. M. (Eds.), Plates, Plumes and Planetary Processes, Geol. Soc. Am., Spec. Paper, 430, 693-722, doi:10.1130/2007.2430(32).

Keskin, M., J. A. Pearce, and J. G. Mitchell (1998). Volcano-stratigraphy and geochemistry of collision-related volcanism on the Erzurum-Kars Plateau, North-eastern Turkey, J. Volcanol. Geotherm. Res., 85, 355-404.

Kurt, M. A., M. Alpaslan, M. C. Göncüoğlu and A. Temel (2008). Geochemistry of late stage medium to high-K calc-alkaline and shoshonitic dykes in the Ulukişla Basin (Central Anatolia, Turkey): Petrogenesis and tectonic setting, Geochem. Int., 46, 1145-1163, doi:10.1134/S0016702908110062.

Kurum, S. and T. Baykara (2020). Geochemistry of post-collisional Yolçatı (Bingöl) volcanic rocks in Eastern Anatolia, Turkey, J. Afr. Earth Sci., 161, 103653, doi:10.1016/j.jafrearsci.2019.103653.

Le Bas, M. J., R. W. Le Maitre, A. Streckeisen and B. Zanettin (1986). A chemical classification of volcanic rocks based on the total alkali-silica diagram, J. Petrol., 27(3), 745-750, doi:10.1093/petrology/27.3.745.

Le Pichon, X. and J. M. Gaulier (1988). The rotation of Arabia and the Levant fault system, Tectonophysics, 153, 271-294.

Lippolis, C. (2020). L'area archeologica di Tūlūl Al-Baqarat. Gli scavi della missione italiana, Apice Libri, Sesto Fiorentino (Firenze), I-II, 454, ISBN: 978-88-99176-98-3.

Lustrino, M., G. Salari, B. Rahimzadeh, L. Fedele et al. (2021). Quaternary melanephelinites and melilitites from Nowbaran (NW Urumieh-Dokhtar Magmatic Arc, Iran): origin of ultrabasic-ultracalcic melts in a post-collisional setting, J. Petrol., 62 9, egab058, doi:10.1093/petrology/egab058.

Macdonald, R. (1974). Nomenclature and petrochemistry of the peralkaline oversaturated extrusive rocks, Bull. Volcanol., 38, 498-516.

McKenzie, D. P., D. Davies and P. Molnar (1970). Plate tectonics of the Red Sea and East Africa, Nature, 226, 243-248.

Nouri, F., H. Azizi, J. Golonka, Y. Asahara et al. (2016). Age and petrogenesis of Na-rich felsic rocks in western Iran: Evidence for closure of the southern branch of the Neo-Tethys in the Late Cretaceous, Tectonophysics, 671, 7, 151-172.

Oddone, M., Z. Yegingil, M. Ozdogan, S. Meloni et al. (2003). Provenance studies of obsidian artefacts from Turkish Neolithic sites using an interdisciplinary approach INAA and Fission Track Dating, Rev. Archéométrie, 27, 137-145, doi:10.3406/arsci.2003.1049.

Özdemir, Y., Ö. Karaoğlu, A. U. Tolluoğlu and N. Güleç (2006). Volcanostratigraphy and petrogenesis of the Nemrut stratovolcano, East Anatolian High Plateau: the most recent post-collisional volcanism in Turkey, Chem. Geol., 226, 189-211, doi:10.1016/j.chemgeo.2007.07.012.

Özdogan, M. (1994). Çayônii: the chipped stone industry of the Pottery Neolithic layers, in Neolithic Chipped Stone Industries of the Fertile Crescent, H. G. Gebel and S. K. Kozlowski (Eds.), Berlin, 267-277.

Pearce, J. A., J. F. Bender, S. E. De Long, W. F. S. Kidd et al. (1990). Genesis of collision volcanism in Eastern Anatolia, Turkey, J. Volcanol. Geotherm. Res., 44, 189-229, doi:10.1016/0377-0273(90)90018-B.

Poidevin, J. L. (1998). Les gisements d'obsidienne de Turquie et de Transcaucasie: géologie, géochimie et chronométrie, in L'obsidienne au Proche et Moyen-Orient: Du Volcan à l'Outil, M. C. Cauvin, A. Gourgaud, B. Gratuze, N. Arnaud, G. Poupeau, J. L. Poidevin et al. (Eds.), BAR Int. Ser., 105-167.

Quinlan, J. R. (1986). Induction of Decision Trees, Mach. Learn., 1, 81-106.

Quinlan, J. R. (2014). C4.5: Programs for Machine Learning, Elsevier, 58-60.

Robertson, A. H. F. (2000). Tectonic evolution of Cyprus in its easternmost Mediterranean setting, in Proceedings Third International Conference on the Geology of the Eastern Mediterranean, Geological Survey Department, Cyprus Ministry of Agriculture, Natural Resources and Environment, Nicosia, Cyprus, 11-44.

Robin, A. K., D. Mouralis, E. Akköprü, B. C. Gratuze et al. (2016). Identification and characterization of two new obsidian sub-sources in the Nemrut volcano (Eastern Anatolia, Turkey): The Sıcaksu and Kayacık obsidian, J. Archaeol. Sci. Rep., 9, 705-717, doi:10.1016/j.jasrep.2016.08.048.

Schmincke, H. U. and M. Sumita (2014). Impact of volcanism on the evolution of Lake Van (Eastern Anatolia) III: periodic (Nemrut) vs. episodic (Suphan) explosive eruptions and climate forcing reflected in a tephra gap between ca. 14 ka and ca. 30 ka, J. Volcanol. Geotherm. Res., 285, 195-213, doi:10.1016/j.jvolgeores.2014.08.015.

Şengör, A. M. C. and W. S. F. Kidd (1979). Post-collisional tectonics of the Turkish-Iranian Plateau and a comparison with Tibet, Tectonophysics, 55, 361-376.

Şengör, A. M. C. and Y. Yılmaz (1981). Tethyan evolution of Turkey: A plate tectonic approach, Tectonophysics, 75, 181-241.

Şengör, A. M. C., S. Özeren, T. Genç and E. Zor (2003). East Anatolian high plateau as a mantle-supported, north-south shortened domal structure, Geophys. Res. Lett., 30, 8045, doi:10.1029/2003GL017858.

Şengör, A. M. C., M. S. Özeren, M. Keskin, M. Sakınç et al. (2008). Eastern Turkish high plateau as a small Turkic-type orogen: Implications for post-collisional crust-forming processes in Turkic-type orogens, Earth-Sci. Rev., 90, 1-2, 1-48, doi:10.1016/j.earscirev.2008.05.002.

SharpLearning, An opensource machine learning library for C# .Net. (https://github.com/mdabros/SharpLearning).

Shaw, J. E., J. A. Baker, M. A. Menzies, M. F. Thirlwall et al. (2003). Petrogenesis of the largest intraplate volcanic field on the Arabian plate (Jordan): a mixed lithosphere asthenosphere source activated by lithospheric extension, J. Petrol., 44, 1657-1679, doi:10.1093/petrology/egg052.

Sumita, M. and H. U. Schmincke (2013). Impact of volcanism on the evolution of Lake Van I: evolution of explosive volcanism of Nemrut volcano (eastern Anatolia) during the past >400,000 years, Bull. Volcanol., 75, 714, doi:10.1007/s00445-013-0714-5.

Tykot, R. H. (1996). Obsidian procurement and distribution in the central and western Mediterranean, J. Mediterr. Archaeol., 9, 1, 39-82, doi:10.1558/jmea.v9i1.39.

Tykot, R. H. (2002). Chemical fingerprinting and source tracing of obsidians, Acc. Chem. Res., 35(8), 618-627.

Vaggelli, G. and R. Cossio (2012). μ-XRF analysis of glasses: a non-destructive utility for cultural heritage applications, Analyst, 137, 662-667, doi:10.1039/c1an15518k.

Vaggelli, G., V. Lovera, R. Cossio and P. Mirti (2013). Islamic glass weights from Egypt: a systematic study by non-destructive μ-XRF technique, J. Non-Cryst. Solids, 363, 96-102, doi:10.1016/j.jnoncrysol.2012.12.003.

Vaggelli, G., R. Cossio, A. Borghi and C. Lippolis (2020). Studio archeometrico di alcune lame in ossidiana da Tūlūl al-Baqarat – TB7, in L'Area Archeologica di Tūlūl Al-Baqarat. Gli scavi della missione italiana, Apice Libri, Sesto Fiorentino, 2, 451-454, ISBN:978-88-99176-98-3.

Vaggelli, G., R. Cossio, A. Borghi, S. Ghignone and C. Lippolis (2025). Geochemistry-based Machine Learning approach applied to archaeological provenance study: the obsidian blades of Tulūl al-Baqarat (Iraq). Front. Earth Sci., doi:10.3389/feart.2025.1675908.

Westaway, R. (2003). Kinematics of the Middle East and eastern Mediterranean updated, Turk. J. Earth Sci., 12, 5-46.

Yılmaz, Y. (1993). New evidence and model on the evolution of the Southeast Anatolian Orogen, Geol. Soc. Am. Bull., 105, 2, 251-271.

Yılmaz, Y., Y. Güner and F. Şaroğlu (1998). Geology of the Quaternary volcanic centres of the East Anatolia, J. Volcanol. Geotherm. Res., 85, 173-210, doi:10.1016/S0377-0273(98)00055-9.

***CORRESPONDING AUTHOR: Gloria VAGGELLI**,
Istituto di Geoscienze e Georisorse, CNR, Via Valperga Caluso, 35, I-10123 Torino
e-mail: gloria.vaggelli@igg.cnr.it